

## Surface Science of Soft Scorpionates

Dawn Wallace, Edward J. Quinn, David R. Armstrong, John Reglinski,\* Mark D. Spicer,\* and W. Ewen Smith

*WestChem, Department of Pure & Applied Chemistry, University of Strathclyde, 295 Cathedral Street, Glasgow, G1 1XL, U.K.*

Received July 27, 2009

The chemisorption of the soft scorpionate  $\text{Li}[\text{PhTm}^{\text{Me}}]$  onto silver and gold surfaces is reported. Surface enhanced Raman spectroscopy in combination with the Raman analysis of suitable structural models, namely,  $[\text{Cu}(\kappa^3\text{-S,S,S-PhTm}^{\text{Me}})(\text{PCy}_3)]$ ,  $[\text{Ag}(\kappa^3\text{-S,S,S-PhTm}^{\text{Me}})(\text{PCy}_3)]$ ,  $[\text{Ag}(\kappa^2\text{-S,S-PhTm}^{\text{Me}})(\text{PEt}_3)]$ , and  $[\text{Au}(\kappa^1\text{-S-PhTm}^{\text{Me}})(\text{PCy}_3)]$ , are employed to identify the manner in which this potentially tridentate ligand binds to these surfaces. On colloidal silver surface-enhanced Raman spectroscopy (SERS) spectra are consistent with  $\text{PhTm}^{\text{Me}}$  binding in a didentate fashion to the surface, holding the aryl group in close proximity to the surface. In contrast, on gold colloid, we observe that the species prefers a monodentate coordination in which the aryl group is not in close proximity to the surface.

### Introduction

Colloids prepared from silver and gold have become extremely important in analytical biotechnology and trace analysis.<sup>1</sup> Their use in combination with vibrational spectroscopy, particularly surface enhanced resonance Raman spectroscopy (SERRS), allows the detection of analytes such as DNA and explosives present at very low concentrations ( $\sim 10^{-12}$ – $10^{-13}$  M) in complex and heterogeneous samples.<sup>2</sup> However, the detection of these species is highly dependent on the analyte adhering to the roughened metal surface.<sup>3</sup> These interactions are typically sustained by polar forces or the dielectric constant of the surface layer. However, if the analyte does not contain a suitable functional group (e.g.,

pyridine, benzotriazole) with which it can form a durable interaction with the surface, it is common to provide a surface modifier which assists the binding process.<sup>1–3</sup> The nature of the surface modifiers commonly used reflect the nature of the analyte. As such, citrate is widely used for proteins,<sup>4</sup> spermine for DNA,<sup>5</sup> and thiolates for the fabrication of self-assembled monolayers.<sup>6</sup> While citrate and spermine are highly stable species, thiolates can be prone to oxidation and surface migration. Thus, although sulfur donors are acknowledged to be highly compatible with the noble metal surfaces used in many of the current applications of colloid technology, their chemical behavior can be expected to affect commercial application as the drive for precision, accuracy, reproducibility, and longevity increases.

The unwanted reactivity of the sulfur atom in thiolate based surface modifiers can be reduced by using alternative sulfur based functional groups such as disulfides, thioethers, dithiocarbamates, and thiones.<sup>7</sup> The latter attracted our attention some years ago as a result of our interest in the chemistry of sulfur based tripodal thione donors species

\*To whom correspondence should be addressed. E-mail: j.reglinski@strath.ac.uk (J.R.); m.d.spicer@strath.ac.uk (M.D.S.). Phone: 44-141-548-2349/2800. Fax 44-141-548-4822.

(1) (a) Ryder, A. G.; O'Connor, G. M.; Glynn, T. J. *J. Raman Spectrosc.* **2000**, *31*, 221–227. (b) Sagmüller, B.; Schwarze, B.; Brehm, G.; Schneider, S. *Analyst* **2001**, *126*, 2066–2071. (c) Faulds, K.; Smith, W. E.; Graham, D.; Lacey, R. J. *Analyst* **2002**, *127*, 282–286.

(2) (a) Storhoff, J. J.; Elghanian, R.; Mucic, R. C.; Mirkin, C. A.; Letsinger, R. L. *J. Am. Chem. Soc.* **1998**, *120*, 1959–1964. (b) Faulds, K.; Smith, W. E.; Graham, D. *Anal. Chem.* **2004**, *76*, 412–417. (c) Faulds, K.; Smith, W. E.; Graham, D. *Analyst* **2005**, *130*, 1125–1131. (d) Faulds, K.; Barbagallo, R. P.; Keer, J. T.; Smith, W. E.; Graham, D. *Analyst* **2004**, *129*, 567–568.

(3) (a) Kneipp, K.; Wang, Y.; Dasari, R. R.; Feld, M. S.; Gilbert, B. D.; Janni, J. A.; Steinfeld, J. I. *Spectrochim. Acta A* **1995**, *51*, 2171–2175. (b) Sands, H. S.; Hayward, I. P.; Kirkbride, T. E.; Bennet, R.; Lacey, R. J.; Batchelder, D. N. *J. Forensic Sci.* **1998**, *43*, 509–513. (c) Sylvia, J. M.; Janni, J. A.; Klein, J. D.; Spencer, K. M. *Anal. Chem.* **2000**, *72*, 5834–5840. (d) McHugh, C. J.; Keir, R.; Graham, D.; Smith, W. E. *Chem. Commun.* **2002**, 580–581.

(4) (a) Rospendowski, B. N.; Kelly, K.; Wolf, C. R.; Smith, W. E. *J. Am. Chem. Soc.* **1991**, *113*, 1217–1225. (b) Picorel, R.; Chumanov, G.; Cotton, T. M.; Montoya, G.; Toon, S.; Seibert, M. J. *Phys. Chem.* **1994**, *98*, 6017–6022. (c) Macdonald, I. D. G.; Smith, W. E. *Langmuir* **1996**, *12*, 706–713. (d) Pearman, W. F.; Lawrence-Snyder, M.; Angel, S. M.; Decho, A. W. *Appl. Spectrosc.* **2007**, *61*, 1295–1300.

(5) (a) Graham, D.; Faulds, K. *Chem. Soc. Rev.* **2008**, *37*, 1042–1051. (b) Faulds, K.; McKenzie, F.; Smith, W. E.; Graham, D. *Angew. Chem., Int. Ed.* **2007**, *46*, 1829–1831. (c) Faulds, K.; Smith, W. E.; Graham, D. *Anal. Chem.* **2004**, *76*, 412–417. (d) Graham, D.; Mallinder, B. J.; Smith, W. E. *Biopolymers* **2000**, *57*, 85–91.

(6) (a) Krolkowska, A.; Bukowska, J. *J. Raman Spectrosc.* **2007**, *38*, 936–942. (b) Srisombat, L. O.; Park, J. S.; Zhang, S.; Lee, T. R. *Langmuir* **2008**, *24*, 7750–7754. (c) Zhang, F.; Skoda, M. W. A.; Jacobs, R. M. J.; Drensen, D. G.; Martin, R. A.; Martin, C. M.; Clark, G. F.; Lamkemeyer, T.; Schreiber, F. *J. Phys. Chem.* **2009**, *113*, 4839–4847.

(7) (a) Chung, Y. C.; Chiu, Y. H.; Wu, Y. W.; Tao, Y. T. *Biomaterials* **2005**, *26*, 2313–2324. (b) Mekhalif, Z.; Fonder, G.; Auguste, D.; Laffineur, F.; Delhalle, J. *J. Electroanal. Chem.* **2008**, *618*, 24–32. (c) Ito, E.; Noh, J.; Hara, M. *Surf. Sci.* **2008**, *602*, 3291–3296. (d) Long, D. P.; Troisi, A. *J. Am. Chem. Soc.* **2007**, *129*, 15303–15310. (e) Shervedani, R. K.; Hatefi-Mehrdadi, A.; Babadi, M. K. *Electrochim. Acta* **2007**, *52*, 7051–7060.

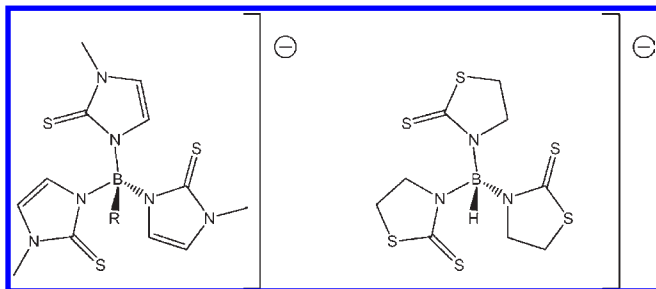


**Figure 1.** Structure of tris(methimazolyl)borato ( $R = H, Ph$ ;  $Tm^{Me}$ ,  $PhTm^{Me}$ ) and tris(thiazolyl)borato anions ( $Tz$ ).<sup>8</sup>

( $Tm^{Me}$ ,  $Tz$ ; Figure 1).<sup>8</sup> These borate based tripodal species contain a negative charge which is not centered on the sulfur donors. It is thus possible to maintain an interaction between the thione modifier and the metal surface but to limit the problematic redox properties found in many sulfur donors (e.g., thiolates). Furthermore, these species are polydentate and thus can, potentially, have a larger footprint on the colloid surface than the unidentate thiolate species currently used, mitigating problems of modifier migration on the surface.

In our previous study<sup>9</sup> on the use of silver colloid with  $Tm^{Me}$  and  $Tz$  (Figure 1) we used hemin to show that these species had attached to the surface and that they performed as surface modifiers. Hemin alone is not readily adsorbed onto colloid surfaces and normally does not give surface enhanced Raman spectra. In the presence of our surface modifying ligands, however, surface enhancement was observed suggesting that it interacts with the modifier. It was further inferred that the modifier was bonded to the surface in a didentate mode leaving a thione donor group free to interact with the hemin thus tethering it close enough to the surface for enhancement to occur. Since this preliminary

report on the deposition of  $Tm^{Me}$  and  $Tz$  on silver colloid,<sup>9</sup> the chemistry of this ligand system, including their reactions with the coinage metals, has advanced markedly.<sup>10,11</sup> The coordination chemistry of  $RTm^R$  with gold, silver, and copper indicate that the relationship of the ligand to this group of metals follows the expected trend. It forms monodentate complexes with gold, trigonal and tetradentate complexes with silver and copper. Crucially a small number of novel dimetallic and trimetallic species have now been reported (Figure 2).<sup>11</sup> These complexes are viable models for the manner in which these species might deposit on surfaces whereby the donor thiones distribute themselves among adjacent metals. However, this chemistry also suggests that these ligands will interact differently with colloids of different metals.

Concurrent with our preliminary studies using silver colloid, Santos et al. reported the synthesis of  $PhTm^{Me}$  (Figure 1) which has an aryl group bonded to the apical boron.<sup>12</sup> This modification introduces a valuable reporting moiety directly onto the boron which should be detected by vibrational analysis. Coupling our increased understanding of the coinage metal coordination chemistry of these species with the availability of a suitable spectral marker, it should now be possible to investigate the deposition of these species on surfaces, assign their complexation modes and probe the differences which occur between gold and silver. The increased footprint of these tripodal species suggested that we should extend this survey to copper in the hope that this material may be stabilized in colloidal form.

## Experimental Section

All experiments were carried out using standard apparatus and commercially available chemicals except for  $[Cu(PCy_3)_2Cl]$ ,  $[Ag(PCy_3)_2Cl]$ , and  $[Au(PCy_3)Cl]$  which were synthesized according to literature methods.<sup>13</sup> Unless otherwise

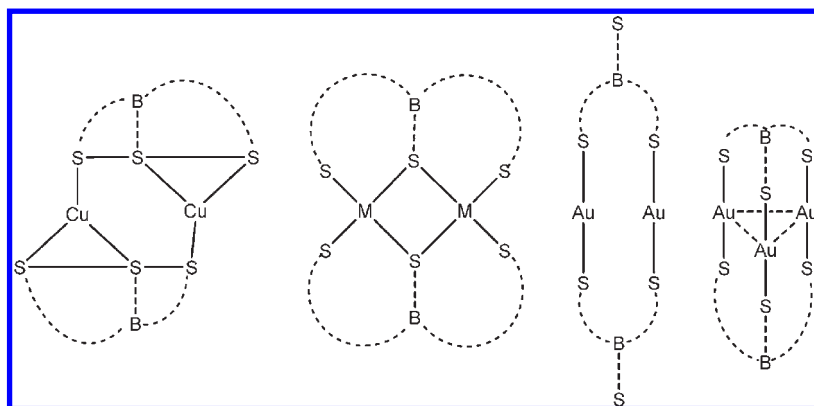


**Figure 2.** Schematic representations of the di and trimetallic complexes of  $RTm^R$ . The dotted lines represent the imidazolyl units which connect the boron to the thione donors.<sup>11</sup>

(8) (a) Reglinski, J.; Garner, M.; Cassidy, I. D.; Slavin, P. A.; Spicer, M. D.; Armstrong, D. R. *J. Chem. Soc., Dalton Trans.* **1999**, 2119–2126. (b) Ojo, J. F.; Slavin, P. A.; Reglinski, J.; Garner, M.; Spicer, M. D.; Kennedy, A. R.; Teat, S. J. *Inorg. Chim. Acta* **2001**, *313*, 15–20. (c) Spicer, M. D.; Reglinski, J. *Eur. J. Inorg. Chem.* **2009**, 1553–1574.

(9) Reglinski, J.; Spicer, M. D.; Ojo, J. F.; McAnally, G. D.; Skórska, A.; Smith, S. J.; Smith, W. E. *Langmuir* **2003**, *19*, 6336–6338.

(10) (a) Effendy; Lobbia, G. G.; Marchetti, F.; Pellei, M.; Pettinari, C.; Pettinari, R.; Santini, C.; Skelton, B. W.; White, A. H. *Inorg. Chim. Acta* **2004**, *357*, 4247–4256. (b) Santini, C.; Pettinari, C.; Lobbia, G. G.; Spagna, R.; Pellei, M.; Vallorani, F. *Inorg. Chim. Acta* **1999**, *285*, 81–88. (c) Bailey, P. J.; Dawson, A.; McCormack, C.; Moggach, S. A.; Oswald, I. D. H.; Parsons, S.; Rankin, D. W. H.; Turner, A. *Inorg. Chem.* **2005**, *44*, 8884–8898. (d) Lobbia, G. G.; Pettinari, C.; Santini, C.; Somers, N.; Skelton, B. W.; White, A. H. *Inorg. Chim. Acta* **2001**, *319*, 15–22.

(11) (a) Patel, D. V.; Mihalcik, D. J.; Kreisel, K. A.; Yap, G. A. P.; Zakharov, L. N.; Kassel, W. S.; Rheingold, A. L.; Rabinovich, D. *Dalton Trans.* **2005**, 2410–2416. (b) Effendy; Lobbia, G. G.; Pettinari, C.; Santini, C.; Skelton, B. W.; White, A. H. *Inorg. Chim. Acta* **2000**, *308*, 65–72. (c) Patel, D. V.; Kreisel, K. A.; Yap, G. A. P.; Rabinovich, D. *Inorg. Chem. Commun.* **2006**, *9*, 748–750. (d) Dodds, C. A.; Garner, M.; Reglinski, J.; Spicer, M. D. *Inorg. Chem.* **2006**, *45*, 2733–2741. (e) Minoura, M.; Landry, V. K.; Melnick, J. G.; Pang, K.-L.; Marchio, L.; Parkin, G. *Chem. Commun.* **2006**, 3990–3992.

(12) Garcia, R.; Paulo, A.; Domingos, A.; Santos, I. *Dalton Trans.* **2003**, 2757–2760.

(13) (a) Bowmaker, G. A.; Boyd, S. E.; Hanna, J. V.; Hart, R. D.; Healy, P. C.; Skelton, B. W.; White, A. H. *Dalton Trans.* **2002**, 2722–2730. (b) Bowmaker, G. A.; Effendy; Harvey, P. J.; Healy, P. C.; Skelton, B. W.; White, A. H. *Dalton Trans.* **1996**, 2449–2457. (c) Jones, P. G.; Sheldrick, G. M.; Muir, J. A.; Muir, M. M.; Pulgar, L. B. *Dalton Trans.* **1982**, 2113–2125.

Table 1. Crystallographic Data

empirical formula	C <sub>36</sub> H <sub>53</sub> BCu- PN <sub>6</sub> S <sub>3</sub>	C <sub>38</sub> H <sub>54.5</sub> AgB- N <sub>6.5</sub> O <sub>0.25</sub> PS <sub>3</sub>
formula weight	771.39	852.19
temperature	120(2) K	123(2) K
wavelength	0.71073 Å	0.71073 Å
crystal system	triclinic	triclinic
space group	<i>P</i> $\bar{1}$	<i>P</i> $\bar{1}$
unit cell dimensions		
<i>a</i> /Å	9.8533(2)	15.0658(2)
$\alpha$ /deg	90.410(1)	78.009(1)
<i>b</i> /Å	10.0078(2)	15.8277(3)
$\beta$ /deg	94.723(1)	85.861(1)
<i>c</i> /Å	19.8773(4)	18.2787(4)
$\gamma$ /deg	106.028(1)	83.389(1)
volume, Å <sup>3</sup>	1876.59(7)	4230.00(13)
<i>Z</i>	2	4
absorption coefficient, mm <sup>-1</sup>	0.827	0.695
reflections collected	37707	37740
independent reflections	8616 [ <i>R</i> (int) = 0.0608]	19400 [ <i>R</i> (int) = 0.0367]
goodness-of-fit on <i>F</i> <sup>2</sup>	1.031	0.979
final <i>R</i> indices	<i>R</i> 1 = 0.0411, w <i>R</i> 2 = 0.0915	<i>R</i> 1 = 0.0378, w <i>R</i> 2 = 0.0994
<i>I</i> > 2σ( <i>I</i> )		
no of parameters	436	944

stated reactions and recrystallizations were carried out in air using commercially available solvents and chemicals. <sup>1</sup>H and <sup>13</sup>C NMR data were acquired at ambient temperature on Bruker DPX or AVANCE NMR spectrometers operating at a proton resonance frequency of 400.13 MHz. Crystals for X-ray analysis were coated in mineral oil and mounted on glass fibers. Data were collected at 120 K on a Nonius Kappa CCD diffractometer using graphite monochromated Mo/*K*α radiation. The heavy atom positions were determined by Patterson synthesis (Au) and direct methods (Ag, Cu), and the remaining atoms located in difference electron density maps. Full matrix least-squares refinement was based on *F*<sup>2</sup>, with all non-hydrogen atoms anisotropic. While hydrogen atoms were mostly observed in the difference maps, they were placed in calculated positions riding on the parent atoms. The structure solution and refinement used the programs SHELX-86, SHELX-97,<sup>14</sup> and the graphical interface WinGX.<sup>15</sup> A summary of the crystallographic parameters are shown in Table 1.

Vibrational spectra were collected using either the 514 nm line of a Spectra Physics argon ion laser coupled with a Renishaw inVia Raman microscope or the 632 nm line of a Spectra Physics helium–neon laser coupled with a Renishaw inVia Raman microscope. All spectra were acquired using approximately 20 mW laser power, three 10 s accumulations, and a 50× long working distance Olympus microscope objective. Each spectrum was normalized against a silicon reference and baseline corrected using GRAMS software.

**Synthesis of [Cu(PhTm<sup>Me</sup>)(PCy<sub>3</sub>)].** LiPhTm<sup>Me</sup> (66 mg, 0.15 mmol) was dissolved in MeOH (10 mL), and [Cu(PCy<sub>3</sub>)<sub>2</sub>Cl] (100 mg, 0.15 mmol) was added. The reaction was stirred at room temperature for 1 h. The white solid was filtered. Yield: 78 mg, (67%). X-ray quality crystals were grown by slow vapor diffusion of CHCl<sub>3</sub>/Et<sub>2</sub>O. Anal. Calcd for C<sub>36</sub>H<sub>53</sub>BCuN<sub>6</sub>PS<sub>3</sub>: C, 56.05; H, 6.93; N, 10.89. Found: C, 56.01; H, 7.27; N, 10.85. <sup>1</sup>H NMR (CDCl<sub>3</sub>, 400 MHz): δ 7.58 (d, 2H, Ph), 7.25 (m, 3H, Ph), 6.81 (d, 3H, CH), 6.65 (d, 3H, CH), 3.56 (s, 9H, CH<sub>3</sub>), 1.78

(br m, 15H, Cy), 1.23 (br m, 15H, Cy). <sup>13</sup>C NMR (CDCl<sub>3</sub>, 100 MHz): δ 162.8 (s, >C=S), 134.9 (s, Ph), 128.2 (s, Ph), 127.1 (s, Ph), 126.7 (s, Ph), 123.4 (s, CH), 117.6 (s, CH), 34.8 (s, CH<sub>3</sub>), 32.5 (d, Cy, *J*(<sup>31</sup>P, <sup>13</sup>C) 44.0 Hz), 30.3 (d, Cy, *J*(<sup>31</sup>P, <sup>13</sup>C) 16.0 Hz), 27.8 (d, Cy, *J*(<sup>31</sup>P, <sup>13</sup>C) 44.0 Hz), 26.6 (s, Cy). <sup>31</sup>P NMR (CDCl<sub>3</sub>, 161 MHz): δ -11.3 (br).

**Synthesis of [Ag(PhTm<sup>Me</sup>)(PCy<sub>3</sub>)].** Because of the light sensitive nature of silver compounds the reaction and subsequent crystallization were carried out in vessels covered with aluminum foil. LiPhTm<sup>Me</sup> (81 mg, 0.19 mmol) was dissolved in MeOH (10 mL), and [Ag(PCy<sub>3</sub>)<sub>2</sub>Cl] (107 mg, 0.15 mmol) was added. The reaction was stirred at room temperature for 12 h. The white solid was filtered. Yield: 101 mg, (65%). X-ray quality crystals were grown by slow vapor diffusion of CH<sub>3</sub>CN/Et<sub>2</sub>O. Anal. Calcd for C<sub>36</sub>H<sub>53</sub>AgBN<sub>6</sub>S<sub>3</sub>·1/2CH<sub>3</sub>CN·1/4Et<sub>2</sub>O: C, 53.55; H, 6.44; N, 10.68; S, 11.29. Found: C, 53.20; H, 7.02; N, 10.77; S, 11.97. <sup>1</sup>H NMR (CD<sub>3</sub>CN, 400 MHz): δ 7.04 (br m, 2H, Ph), 6.93 (br m, 3H, Ph), 6.62 (br d, 3H, CH), 6.58 (br d, 3H, CH), 3.52 (s, 9H, CH<sub>3</sub>), 1.57 (br m, 15H, Cy), 1.22 (br m, 15H, Cy). <sup>13</sup>C NMR (CD<sub>3</sub>CN, 100 MHz): δ 160.9 (s, C=S), 134.1 (s, Ph), 126.2 (s, Ph), 125.7 (s, Ph), 122.5 (s, CH), 118.8 (s, Ph), 118.2 (s, CH), 34.4 (s, CH<sub>3</sub>), 31.2 (d, Cy, *J*(<sup>31</sup>P, <sup>13</sup>C) = 44.0 Hz), 30.3 (d, Cy, *J*(<sup>31</sup>P, <sup>13</sup>C) = 19.2 Hz), 26.7 (d, Cy, *J*(<sup>31</sup>P, <sup>13</sup>C) = 44.8 Hz), 25.7 (s, Cy). <sup>31</sup>P NMR (CD<sub>3</sub>CN, 161 MHz): δ 34.8 (br d, *J*(<sup>31</sup>P, <sup>107/109</sup>Ag) = 1176.1 Hz).

**Synthesis of [Au(PhTm<sup>Me</sup>)(PCy<sub>3</sub>)].** LiPhTm<sup>Me</sup> (100 mg, 0.23 mmol) was dissolved in MeOH (10 mL) and [Au(PCy<sub>3</sub>)Cl] (118 mg, 0.23 mmol) was added resulting in a color change from colorless to orange. The reaction was stirred at room temperature for 1 h. The off white solid was filtered. Yield: 110 mg, (53%). Anal. Calcd for C<sub>36</sub>H<sub>53</sub>AuBN<sub>6</sub>PS<sub>3</sub>: C, 47.79; H, 5.90; N, 9.29; S, 10.63. Found: C, 47.11; H, 6.10; N, 9.19; S, 10.57. <sup>1</sup>H NMR (CDCl<sub>3</sub>, 400 MHz): δ 7.01 (m, 2H, Ph), 6.81 (br m, 3H, Ph), 6.70 (d, 3H, CH), 6.66 (s, 3H, CH), 3.67 (s, 9H, CH<sub>3</sub>), 2.07–1.75 (br m, 15H, Cy), 1.46–1.22 (br m, 15H, Cy). <sup>13</sup>C NMR (CDCl<sub>3</sub>, 100 MHz): δ 134.7 (s, Ph), 126.6 (s, Ph), 126.1 (s, Ph), 124.9 (s, Ph), 117.6 (s, CH), 115.6 (s, CH), 35.3 (s, CH<sub>3</sub>), 33.6 (d, Cy, *J*(<sup>31</sup>P, <sup>13</sup>C) = 112.0 Hz), 31.0 (s, Cy), 27.2 (d, Cy, *J*(<sup>31</sup>P, <sup>13</sup>C) = 48.0 Hz), 26.0 (s, Cy). The >C=S typically observed at about 160 ppm is too weak to be unequivocally assigned. <sup>31</sup>P NMR (CDCl<sub>3</sub>, 161 MHz): δ 58.2.

**Preparation of Silver Colloid.**<sup>16</sup> In a 1000 mL round-bottom flask, 500 mL of distilled water was heated to 40 °C with a Bunsen burner. A solution of silver nitrate (90 mg in 10 mL distilled water) was added to the water and heated rapidly to 98 °C with constant stirring. Once the solution had reached 98 °C a solution of sodium citrate (110 mg in 10 mL distilled water) was added rapidly, and the solution maintained at 98 °C for 90 min with continuous stirring. The nanoparticles produced were consistent with those reported previously (< 35 nm diameter).<sup>16</sup>

**Preparation of Gold Colloid.**<sup>17</sup> A 50 mg portion of sodium tetrachloroaurate was added to 500 mL of distilled water in a 1000 mL round-bottom flask. The solution was heated to boiling point with constant stirring. A 7.5 mL portion of a 1% solution of trisodium citrate was then added. The temperature of the solution was maintained at boiling point for 15 min and then allowed to cool to room temperature with continuous stirring. The nanoparticles produced were consistent with those reported previously (15–20 nm diameter).<sup>17</sup>

**Surface Enhanced Resonance Raman Spectra.** All colloid samples were prepared and analyzed in microtiter plates with a sample volume of 250 μL by mixing 30 μL of poly-L-lysine

(14) (a) Sheldrick, G. M. *SHELXS-86. Program for crystal structure solution*; University of Göttingen: Göttingen, Germany, 1986. (b) Sheldrick, G. M. *SHELXS-97. Program for crystal structure solution*; University of Göttingen: Göttingen, Germany, 1997.

(15) Farrugia, L. J. *J. Appl. Crystallogr.* **1999**, *32*, 837–838.

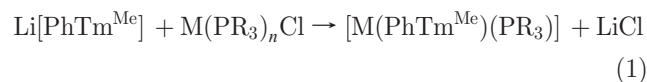
(16) (a) Lee, P. C.; Meisel, D. *J. Phys. Chem.* **1982**, *86*, 3391–3395. (b) Munro, C.; Smith, W. E.; Garner, M.; Clarkson, J.; White, P. C. *Langmuir* **1995**, *11*, 3712–3720. (c) Rodger, C.; Smith, W. E.; Dent, G.; Edmondson, M. *Dalton Trans.* **1996**, 791–799.

(17) Grabar, K. C.; Freeman, R. G.; Hommer, M. B.; Natan, M. J. *Anal. Chem.* **1995**, *67*, 735–743.

(0.01% w/v), 870  $\mu\text{L}$  50:50 (v/v) of colloid/distilled water, and 100  $\mu\text{L}$   $1 \times 10^{-2}$  M ligand solution, giving a final ligand concentration of  $1 \times 10^{-3}$  M.

**Density Functional Theory (DFT) Molecular Orbital Calculations.** Calculations were performed using the Gaussian 03 program.<sup>18</sup> The molecular species were subjected to geometry optimization at the DFT<sup>19</sup> level and the 6-311G\*\* basis set<sup>20</sup> for the atoms C, N, O, S, B, and H. For Silver, the Stuttgart RSC basis set was used.<sup>21</sup> Preliminary calculations were carried out using the DFT functionals BLYP and B3LYP.<sup>22</sup> The best agreement with respect to the experimental Raman frequencies was obtained using the BLYP functionals, and hence these were used for the rest of the molecules.

## Results and Discussion



where M = Cu, R = cyclohexyl,  $n = 2$ ; M = Ag, R = cyclohexyl, ethyl,  $n = 2$ ; M = Au, R = cyclohexyl,  $n = 1$

A series of model complexes, namely,  $[\text{Cu}(\kappa^3\text{-S,S,S-PhTm}^{\text{Me}})(\text{PCy}_3)]$ ,  $[\text{Ag}(\kappa^3\text{-S,S,S-PhTm}^{\text{Me}})(\text{PCy}_3)]$ ,  $[\text{Au}(\kappa^1\text{-S-PhTm}^{\text{Me}})(\text{PCy}_3)]$ , and  $[\text{Ag}(\kappa^2\text{-S,S-PhTm}^{\text{Me}})(\text{PET}_3)]$ , were initially constructed (eq 1). These complexes were designed to provide representative examples of the manner in which these soft tripodal ligands coordinate with coinage metals. Tricyclohexyl- and triethylphosphine were chosen as supporting ligands in these complexes because the ethyl and cyclohexyl groups are not expected to significantly contribute to the Raman spectra especially in the aromatic region and will not be subject to significant enhancement at the colloid surfaces. Since the chemistry of the coinage metals with these species has previously shown great structural variation,<sup>10,11</sup> it was important to structurally characterize the three new

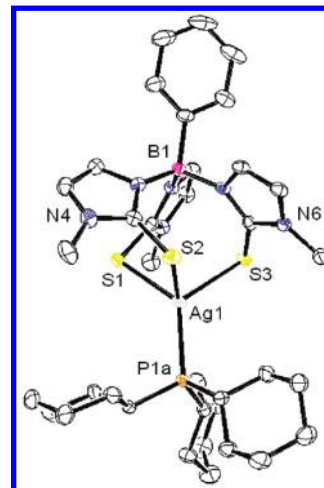


**Figure 3.** X-ray crystal structure of  $[\text{Ag}(\kappa^3\text{-S,S,S-PhTm}^{\text{Me}})(\text{PCy}_3)]$ . The thermal ellipsoids are drawn at 50% probability. The metrical parameters of this complex and its copper analogue can be found in the Supporting Information.

tricyclohexylphosphine ( $\text{PCy}_3$ ) adducts prior to their use as surface modifiers.

Both  $[\text{Cu}(\text{PhTm}^{\text{Me}})(\text{PCy}_3)]$  and  $[\text{Ag}(\text{PhTm}^{\text{Me}})(\text{PCy}_3)]$  were readily crystallized allowing for analysis by X-ray methods (Figure 3). Both complexes have approximately tetrahedral coordination geometry with the ligand adopting a  $\kappa^3\text{-S,S,S}$  coordination mode. The copper complex is isostructural with its triethylphosphine analogue<sup>10d</sup> whereas the silver complex betrays the ambivalent nature of the heavier element in that the  $\text{PhTm}^{\text{Me}}$  ligand in the triethylphosphine complex is didentate resulting in a trigonal planar geometry at the metal. The relationship between these two silver complexes ( $\text{PET}_3$  versus  $\text{PCy}_3$ ) is counterintuitive in that the bulky phosphine displays the higher coordination number. We were unable to obtain suitable crystals of the gold complex,  $[\text{Au}(\text{PhTm}^{\text{Me}})(\text{PCy}_3)]$ , for single crystal X-ray diffraction. However, comparisons with the structurally characterized  $[\text{Au}(\kappa^1\text{-S-Tm}^{\text{Me}})(\text{PET}_3)]$  using spectroscopic methods clearly supports a linear binding mode for this species.

Solid state Raman spectra of  $\text{Li}[\text{PhTm}^{\text{Me}}]$ , tricyclohexylphosphine and the four metal complexes  $[\text{M}(\text{PhTm}^{\text{Me}})(\text{PR}_3)]$  (R = Cy, M = Cu, Ag, Au; R = Et, M = Ag) were recorded (Figure 4). Using DFT calculations the prominent bands in the Raman spectrum of the  $[\text{PhTm}^{\text{Me}}]^-$  anion were assigned as shown in Table 2. Most of the modes are complex in nature, but we have attempted in our assignments to reflect the dominant component. The key vibrational modes are those at  $1565\text{ cm}^{-1}$  which is predominantly an aryl C=C stretch;<sup>23</sup> bands at  $1371$ ,  $1302$ , and  $1283\text{ cm}^{-1}$  which are assigned to C–N stretches in the methimazole rings; a band at  $1001\text{ cm}^{-1}$  which is an aryl ring breathing mode; a band at  $712\text{ cm}^{-1}$  which arises from N–CH<sub>3</sub> stretching and associated methimazole ring breathing; and last a band at  $535\text{ cm}^{-1}$  which is the isolated C=S stretch. The remaining, weaker bands arise from CH<sub>3</sub> deformations ( $1406$ ,  $1453$ , and  $1471\text{ cm}^{-1}$ ) and aryl/methimazole C–H bending modes

(23) The calculations show some methimazole C=C stretching character in the band at  $1565\text{ cm}^{-1}$ , but in the parent  $\text{Tm}^{\text{Me}}$  spectrum the bands in this region of the spectrum are very weak. We believe that in the present case it is likely that these bands are predominantly phenyl C=C stretching in character.

(18) Frisch, M.J.; Trucks, G.W.; Schlegel, H.B.; Scuseria, G.E.; Robb, M.A.; Cheeseman, J.R.; Montgomery, J.A., Jr.; Vreven, T.; Kudin, K.N.; Burant, J.C.; Millam, J.M.; Iyengar, S.S.; Tomasi, J.; Barone, V.; Mennucci, B.; Cossi, M.; Scalmani, G.; Rega, N.; Petersson, G.A.; Nakatsuji, H.; Hada, M.; Ehara, M.; Toyota, K.; Fukuda, R.; Hasegawa, J.; Ishida, M.; Nakajima, T.; Honda, Y.; Kitao, O.; Nakai, H.; Klene, M.; Li, X.; Knox, J.E.; Hratchian, H.P.; Cross, J.B.; Bakken, V.; Adamo, C.; Jaramillo, J.; Gomberts, R.; Stratmann, R.E.; Yazyev, O.; Austin, A.J.; Cammi, R.; Pomelli, C.; Ochterski, J.W.; Ayala, P.Y.; Morokuma, K.; Voth, G.A.; Salvador, P.; Dannenberg, J.J.; Zakrzewski, V.G.; Dapprich, S.; Daniels, A.D.; Strain, M.C.; Farkas, O.; Malick, D.K.; Rabuck, A.D.; Raghavachari, K.; Foresman, J.B.; Ortiz, J.V.; Cui, Q.; Baboul, A.G.; Clifford, S.; Cioslowski, J.; Stefanov, B.B.; Liu, G.; Liashenko, A.; Piskorz, P.; Komaromi, I.; Martin, R.L.; Fox, D.J.; Keith, T.; M. A. Al-Laham, Peng, C.Y.; Nanayakkara, A.; Challacombe, M.; Gill, P.M.W.; Johnson, B.; Chen, W.; Wong, M.W.; Gonzalez, C.; Pople, J.A. *Gaussian 03*, revision B.05; Gaussian, Inc.: Wallingford, CT, 2004.

(19) Kohn, W.; Becke, A. D.; Parr, R. G. *J. Phys. Chem.* **1996**, *100*, 12974–12980.

(20) (a) McLean, A. D.; Chandler, G. S. *J. Chem. Phys.* **1980**, *72*, 5639–5648. (b) Krishnan, R.; Binkley, J. S.; Seeger, R.; Pople, J. A. *J. Chem. Phys.* **1980**, *72*, 650–654.

(21) (a) Dolg, M.; Stoll, H.; Preuss, H.; Pitzer, R. M. *J. Phys. Chem.* **1993**, *97*, 5852. (b) Basis sets were obtained from the Extensible Computational Chemistry Environment Basis Set Database, Version 02/25/04, as developed and distributed by the Molecular Science Computing Facility, Environmental and Molecular Sciences Laboratory which is part of the Pacific Northwest Laboratory, P.O. Box 999, Richland, Washington 99352, U.S.A., and funded by the U.S. Department of Energy. The Pacific Northwest Laboratory is a multi-program laboratory operated by Battelle Memorial Institute for the U.S. Department of Energy under contract DE-AC06-76RLO 1830. Contact David Feller or Karen Schuchardt for further information. <http://www.emsl.pnl.gov/forms/basisform.html>.

(22) (a) Becke, A. D. *Phys. Rev. A.* **1988**, *38*, 3098–3100. (b) Lee, C. T.; Yang, W. T.; Parr, R. G. *Phys. Rev. B.* **1998**, *37*, 785–789.

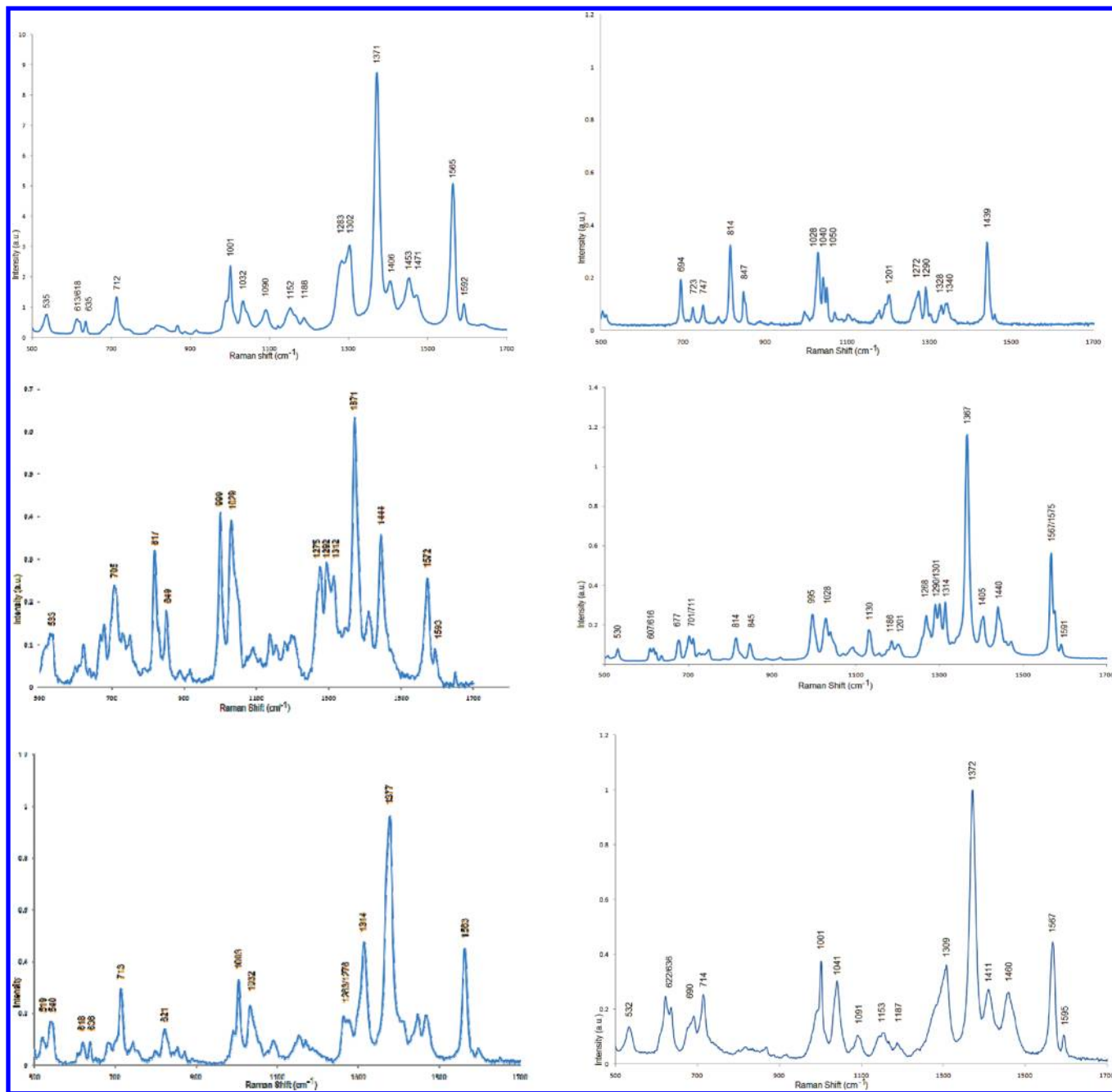


**Figure 4.** Top left: Raman spectrum of solid  $\text{PhTm}^{\text{Mc}}$ , (514 nm, 20 mW). Top right: Raman spectrum of solid  $\text{PCy}_3$ , (514 nm, 20 mW). Middle left: Raman spectrum of solid  $[\text{Cu}(\text{PhTm}^{\text{Mc}})(\text{PCy}_3)]$ , (632 nm, 20 mW). Middle right: Raman spectrum of solid  $[\text{Ag}(\text{PhTm}^{\text{Mc}})(\text{PCy}_3)]$ , (514 nm, 20 mW). Bottom left: Raman spectrum of solid  $[\text{Au}(\text{PhTm}^{\text{Mc}})(\text{PCy}_3)]$ , (632 nm, 20 mW). Bottom right; Raman spectrum of solid  $[\text{Ag}(\text{PhTm}^{\text{Mc}})(\text{PEt}_3)]$ , (632 nm, 20 mW).

(1032–1152  $\text{cm}^{-1}$ ). It is clear from Table 2 that these bands are essentially invariant on complexation, and this has been confirmed by DFT calculations on the silver complexes which show only small shifts in band positions, but do reveal some splitting of bands and changes in intensity. These differences are particularly prominent in the region between 1250 and 1400  $\text{cm}^{-1}$  and are also present in the experimental Raman spectra. This is probably due to the changes in symmetry imposed by the different coordination modes of the ligand. In tridentate,  $\kappa^3$ -coordination, these bands are resolved into a group of three/four, whereas for didentate ( $\kappa^2$ ) and unidentate ( $\kappa^1$ ) forms, which are less geometrically constrained, a broader envelope of bands centered on one dominant frequency is observed.

Silver colloid was modified by addition of  $\text{Li}[\text{PhTm}^{\text{Mc}}]$ , and the SERS spectrum obtained. The spectrum shows that the thione donor has been chemisorbed on the silver surface (Figure 5). The spectrum is again dominated by bands in two frequency ranges, namely, about 1300–1370  $\text{cm}^{-1}$  and about 1550–1650  $\text{cm}^{-1}$ . The band due to the  $>\text{C}=\text{S}$  moiety is very weak, possibly occurring at around 500  $\text{cm}^{-1}$ , a lower frequency than in the complexes, and on the edge of the observed spectral window. This is in keeping with a significant interaction with the surface. The resonances observed for the methimazole rings appear in the expected region; however, their number and distribution is reminiscent of the spectrum of  $[\text{Ag}(\text{PhTm}^{\text{Mc}})(\text{PEt}_3)]$  thus suggesting a didentate binding mode (Figure 4) rather than the tridentate mode

**Table 2.** Key Vibrational Frequencies  $\text{cm}^{-1}$  Derived from  $\text{PhTm}^{\text{Me}}$  As the Free Anion and in Its Complexes with the Coinage Metals<sup>a</sup>

	$\nu(\text{C}=\text{S})$	$\nu(\text{N}-\text{CH}_3)$	$\nu(\text{C}=\text{C})$ (Ph)	$\nu(\text{C}-\text{N})$ (mt)	aromatic
$[\text{PhTm}^{\text{Me}}]^-$	535	712	1001	1283, 1302, 1371	1565
$\text{Cu}(\kappa^3\text{-S,S,S-PhTm}^{\text{Me}})(\text{PCy}_3)$	533	705	999	1275, 1292, 1312, 1371	1572
$\text{Ag}(\kappa^3\text{-S,S,S-PhTm}^{\text{Me}})(\text{PCy}_3)$	530	711	995	1290, 1301, 1314, 1367	1567, 1575
$\text{Ag}(\kappa^2\text{-S,S-PhTm}^{\text{Me}})(\text{PEt}_3)$	532	714	1001	1309 (br) 1372	1567
$\text{Au}(\kappa^1\text{-S-PhTm}^{\text{Me}})(\text{PCy}_3)$	519, 540	713	1000	1263, 1276, 1314, 1377	1563

<sup>a</sup>The assignments were confirmed using DFT calculations.<sup>18–22</sup>

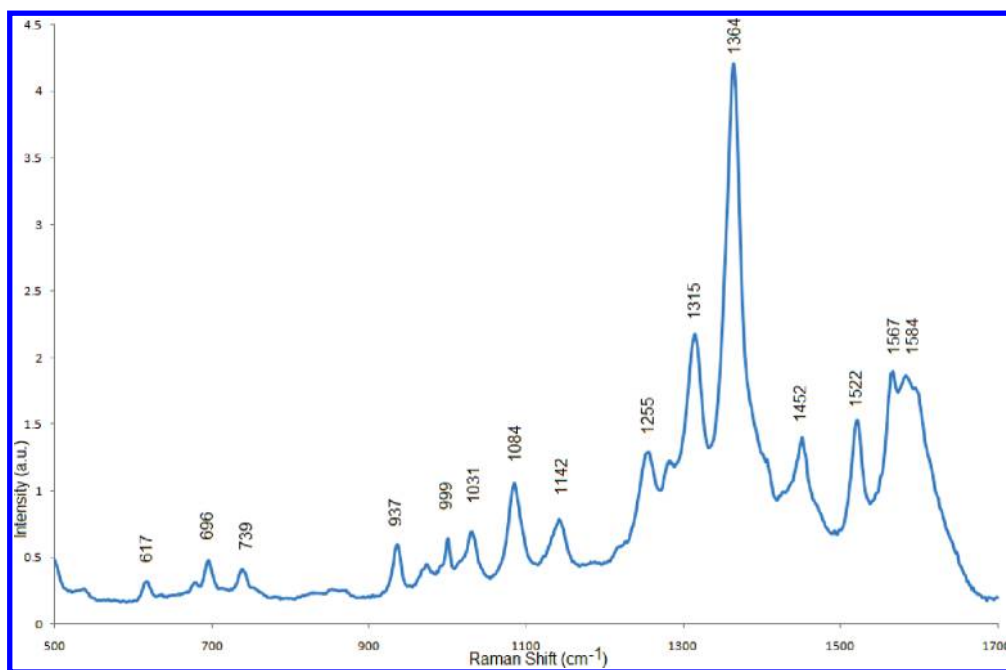


**Figure 5.** SERS spectrum of  $\text{PhTm}^{\text{Me}}$  deposited on silver colloid, (514 nm, 20 mW).

observed in the solid  $\text{PCy}_3$  complex. Furthermore, comparison of the spectra obtained here for the  $\text{PhTm}^{\text{Me}}$  anion with that reported previously for the  $\text{Tm}^{\text{Me}}$  anion reveals a great deal of similarity between the two species when deposited on the silver surface, again suggesting a didentate binding mode for the  $\text{Tm}^{\text{Me}}$  anion on the silver surface.<sup>9</sup> The relative intensity of the band assigned to the aromatic group is greater on surface deposition, and other related vibrations are also enhanced to give a more complex spectrum in this region (Figures 4, 5). This implies that the phenyl group is able to approach the surface sufficiently closely for the associated Raman bands to undergo surface enhancement. The additional bands in this region are likely to be other stretching modes of the phenyl ring system which have been selectively enhanced as a consequence of the surface selection rules of SERS. This provides further evidence that this is indeed a SERS rather than a Raman spectrum, a fact already clear from the intensity of what is effectively a monolayer. In the absence of any symmetry considerations, the basic SERS selection rule states that intense scattering arises from vibrations which involve large changes in polarizability perpendicular to the plane of the surface. At about  $1600\text{ cm}^{-1}$ , if the plane of the molecule is perpendicular to the surface plane, one mode, a quadrant stretch of the phenyl ring, would be dominant as it is in the Raman spectra of the complexes. The fact that a number of modes are enhanced suggests that the phenyl ring is at an angle to the surface or possibly parallel to it.

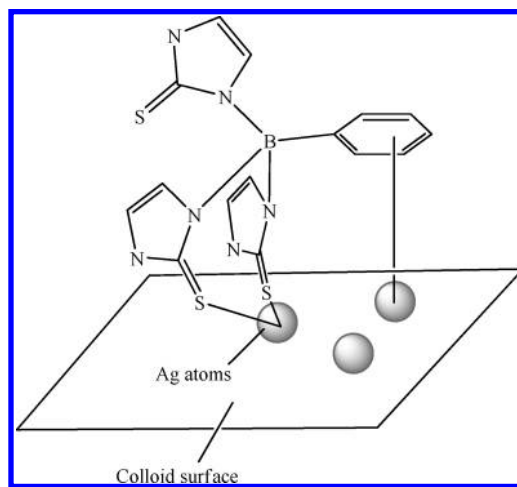


**Figure 6.** Postulated didentate orientation of  $\text{PhTm}^{\text{Me}}$  on Ag colloid surface which facilitates an interaction of the phenyl moiety with the colloid surface.

The SERS spectrum of  $\text{PhTm}^{\text{Me}}$  deposited on gold colloid has only two distinct, high intensity resonances at  $1316\text{ cm}^{-1}$  and  $1367\text{ cm}^{-1}$ . They are of approximately equal strength, and are assigned to vibrations in the methimazole rings (Figure 7). Although the spectrum obtained from  $\text{PhTm}^{\text{Me}}$  deposited on gold colloid and solid  $[\text{Au}(\text{PhTm}^{\text{Me}})(\text{PCy}_3)]$  have roughly coincident bands in this region, their absolute and relative intensities have changed, most probably because

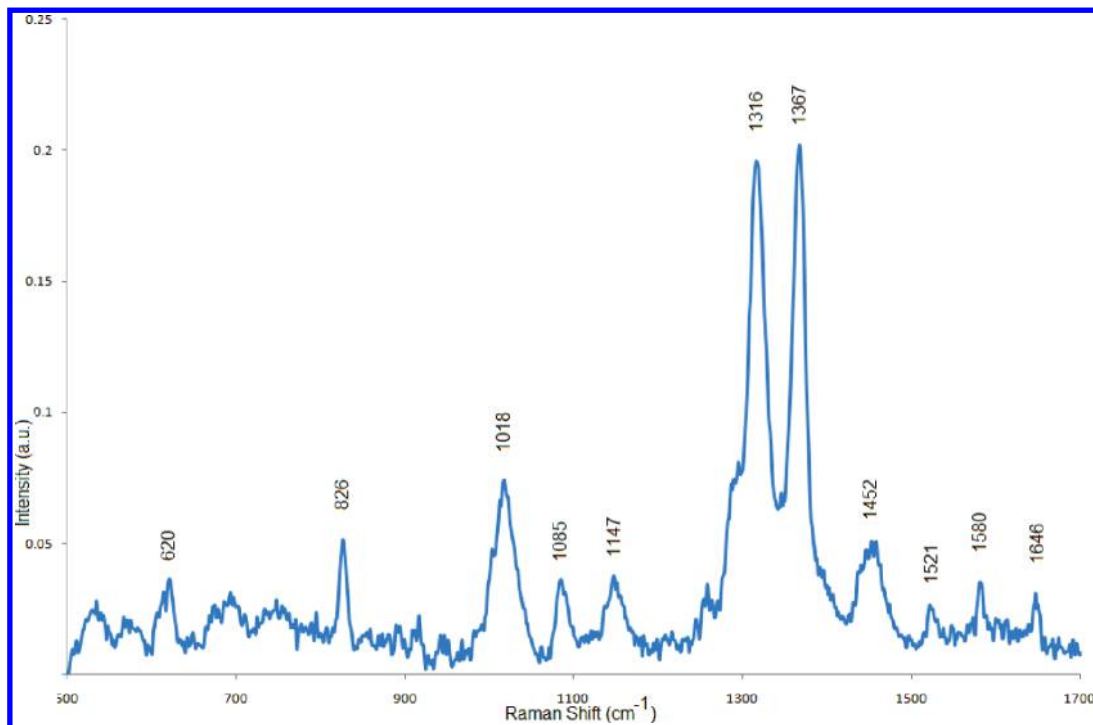


**Figure 7.** SERS spectrum of  $\text{PhTm}^{\text{Me}}$  deposited on gold colloid, (632 nm, 20 mW). The lower signal-to-noise ratio is ascribed to the poorer surface enhancement at gold (cf. silver).

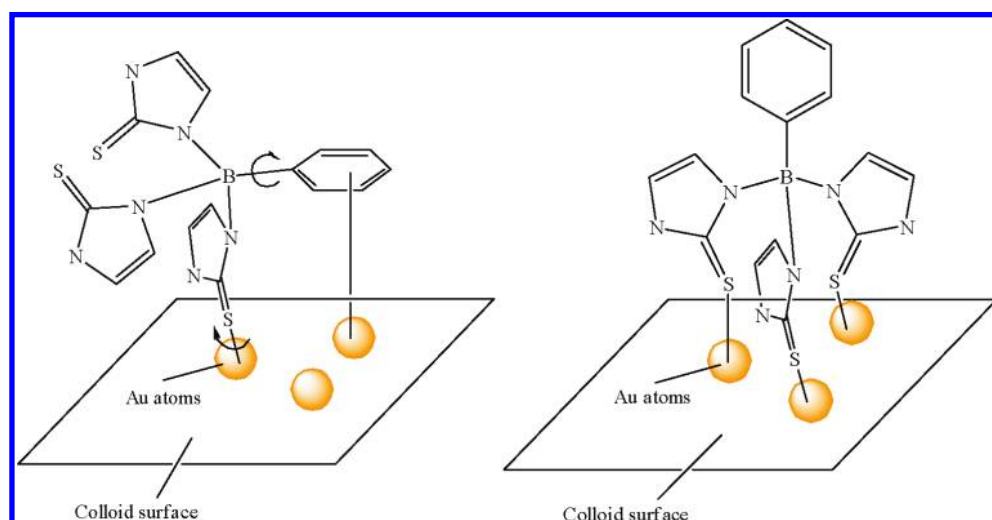


**Figure 8.** Orientations of  $\text{PhTm}^{\text{Me}}$  on gold colloid surface: (left) monodentate on one individual gold atom, (right) monodentate on three individual gold atoms, with the phenyl moiety remote from the colloid surface.

of the influence of the surface. This would indicate that the structure of the solid gold complex, that is, monodentate and linear, is upheld at the colloidal surface (Figure 8). However, this mode of binding potentially allows the phenyl group to come into close proximity with the colloid surface. Thus the absence of a relevant band ( $\sim 1600\text{ cm}^{-1}$ ) suggests that any interaction of this type is very weak because of rapid rotation of  $\text{PhTm}^{\text{Me}}$  on the surface, a process which would be allowed by unidentate coordination. The presence of only one methimazole in close proximity to the surface would also explain the general weakness and breadth of the methimazole bands.

Considering known structures of gold  $\text{R}'\text{Tm}^{\text{R}}$  complexes, an alternative model can be envisaged, where each of the

three sulfur atoms coordinate to a different gold atom on the colloid surface (Figure 8). An overall tridentate coordination mode would be achieved leading to the phenyl group being remote from the surface, reducing the intensity of the aryl resonance in the SERS spectrum. Coordination of  $\text{Tm}^{\text{R}}$  ligands over three separate gold atoms has been demonstrated by Rabinovich in  $[\text{Au}_3(\text{Tm}^{\text{tBu}})_2]$  (Figure 2).<sup>11c</sup> However, this mode of binding requires the inversion of the  $\text{Tm}^{\text{Me}}$  ligand at the boron atom forcing the hydridic proton into the core of the metal triangle. This configuration is not possible for  $\text{PhTm}^{\text{Me}}$  (for obvious steric reasons), and the ligand would thus be forced to adopt a configuration with the phenyl group remote from the surface. Such a configuration would be similar to that of the synthetic models,

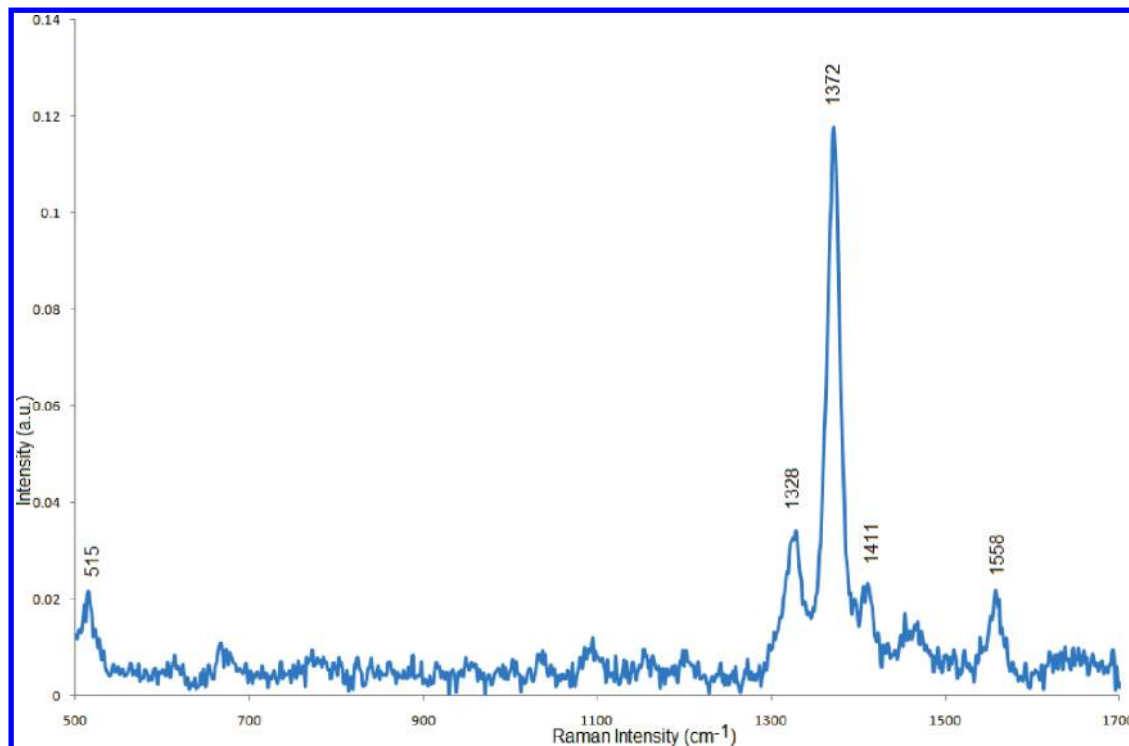


**Figure 9.** SERS spectrum of  $\text{Tm}^{\text{Me}}$  deposited on gold colloid (632 nm, 20 mW).

$[\text{Cu}(\text{PhTm}^{\text{Me}})(\text{PCy}_3)]$  and  $[\text{Ag}(\text{PhTm}^{\text{Me}})(\text{PCy}_3)]$ , except that three metal centers rather than one would be used to achieve binding. This configuration would have a similar symmetry to the two tridentate complexes, and we would thus expect to see a more intense spectrum and bands of disparate intensity between  $1300\text{ cm}^{-1}$  and  $1380\text{ cm}^{-1}$ . However, this structure would also be highly strained, and we consider it unlikely to occur.

To probe this further we also obtained the spectrum of the parent  $\text{Tm}^{\text{Me}}$  anion deposited on gold colloid (Figure 9). The spectrum consists of a single intense band at  $1372\text{ cm}^{-1}$  accompanied by broad, weak bands at approximately  $1327$  and  $1560\text{ cm}^{-1}$ . This seems more closely allied to the spectrum of the didentate ligand on silver colloid. It is possible that the borohydride can interact with the metal surface.<sup>9</sup> This would be a stronger, more directed interaction than that of the phenyl group in  $\text{PhTm}^{\text{Me}}$  and may result in constraint of the methimazoles close to the surface resulting in a didentate mode.

Technologies based on silver and gold colloid are well developed, but copper colloid has not received as much attention because of problems with its stability. We had hoped that the strong affinity of these soft tripodal thione species for copper and their ability to span metal centers (Figure 2) would assist the stabilization of copper colloid. However, despite protracted efforts adding  $\text{Tm}^{\text{Me}}$  and  $\text{PhTm}^{\text{Me}}$  both pre and post colloid formation,<sup>24</sup> we were unable to extend the lifetime of this elusive material.

### Concluding Remarks

The study supports the view that the tripodal thione species  $\text{PhTm}^{\text{Me}}$  and  $\text{Tm}^{\text{Me}}$  are good surface modifiers for silver and gold colloid. However, their relationship with the two metal surfaces is different. With gold the surface modifier is unidentate and with silver it is didentate. It is envisaged that eventually the phenyl group will be replaced by a more apposite sensing molecule or a selective coupling agent. Should detection be linked to surface enhancement then the surface of choice would probably be silver as this study predicts that with this material the analyte would be brought into close proximity to the surface.

**Acknowledgment.** D.W. thanks the EPSRC and University of Strathclyde Doctoral Training Account for financial support.

**Supporting Information Available:** Crystallographic data for  $[\text{Cu}(\kappa^3\text{-S,S,S-PhTm}^{\text{Me}})(\text{P}(\text{Cy})_3)]$  and  $[\text{Ag}(\kappa^3\text{-S,S,S-PhTm}^{\text{Me}})(\text{P}(\text{Cy})_3)]$ . An analysis of the metrical parameters for  $[\text{Cu}(\kappa^3\text{-S,S,S-PhTm}^{\text{Me}})(\text{P}(\text{Cy})_3)]$ ,  $[\text{Ag}(\kappa^3\text{-S,S,S-PhTm}^{\text{Me}})(\text{P}(\text{Cy})_3)]$  and related compounds. Results of DFT studies on  $\text{PhTm}^{\text{Me}}$  and didentate and tridentate silver complexes leading to an assignment of the vibrational spectrum. This material is available free of charge via the Internet at <http://pubs.acs.org>.

(24) Creighton, J. A.; Alvarez, M. S.; Wertz, D. A.; Garoff, S.; Kim, M. W. *J. Phys. Chem.* **1983**, *87*, 4793–4799.